Marine Verongiid Demosponge Lanthella Basta

Subjects: Materials Science, Biomaterials | Nanoscience & Nanotechnology | Marine & Freshwater Biology
Contributor: Ahmet Kertmen

Marine sponges were among the first multicellular organisms on our planet and have survived to this day thanks to their unique mechanisms of chemical defense and the specific design of their skeletons, which have been optimized over millions of years of evolution to effectively inhabit the aquatic environment. *Ianthella basta* (Pallas, 1766) is one of the largest, fan-shaped marine demosponges that can reach up to 2.5 m both in height; and the body of which is a micro-reticular, durable structure that determines the ideal filtration function of this organism. Calcite biomineral is responsible for nano-tuning the chitinous skeletal fibers of this sponge species.

biological materials | demospongiae | biomineralization | calcite | chitin | Micro X-ray Fluorescence | NEXAFS

1. Introduction

Biominerals in unicellular and multicellular organisms serve many functions in both their survival and active metabolic existence. It is not surprising that in a multi-million years of evolutionary process, organisms have developed the ability to use a wide range of different chemical elements to create biominerals. Thus, a variety of organisms sequester not only Ca and Si, but also Au, Zn, Mn, Cr, Ni, V, Fe, into biominerals (see for an overview [1]).

Biomineralization in sponges (Porifera), which were the first multicellular organisms on the planet, remains a focus of modern biomineralogy and bioinspired materials chemistry. Such poriferan classes as Hexactinellida, Demospongia, and Hexascleromorpha include species with silicified skeletal constructs (spicules and frameworks). In some cases, representatives of hexactinellids, or glass sponges, possess nanophases of calcite within their siliceous skeletal structures [2]. Unique silica-aragonite-chitin biocomposites are examples of multiphase biomineralization that have been discovered in selected verongiid demosponges [3]. However, sponges that belong to the Calcarea class are known to construct their hard tissues only from calcium carbonates [4][5]. While evidence for the presence of the aforementioned biominerals in sponges′ skeletons is numerous and indisputable, debate still revolves around understanding the principles of biomineralization and corresponding mechanisms at the molecular level. Particular attention is paid to the identification of proteins (i.e., silicateins, glassin, cathepsins, collagens) [6][7][8][9] and polysaccharides (i.e., chitin) [10][11] that act as templates for the formation of silica-based mineral phases. The forehead sponge body is a soft and elastic organic matter resting on the mineral skeleton of a particular physical form. This functional biological 3D construct is designed to extract appropriate feed from the

aquatic environment by filtration using micro- and macropores with maximum efficiency. Accordingly, the mineralization of the sponge skeleton contributes to an increase in the total area of the filtering surface and the adoption of an optimal position for the sponge body in water, being attached to a solid substrate. At the same time, the ability of this sponge to maintain a vertical position in water space, being firmly attached to the substrate (**Figure 1**), logically suggests the presence of some kind of “cementing” component inside this structure. Appearance of micro-bubbles after insertion of this sponge into acidic solutions can be regarded as indication of existence of calcium carbonate within the sponge body. Indeed, this visual observation has been backed up by spectroscopic and microscopic imaging methods.

Figure 1. Marine verongiid demosponge Ianthella basta possess a huge chitin-based, a network-like skeleton that is stiff enough to withstand underwater currents due to its natural rigidity.

2. Identification of Ca and Br Localization Using Three-Dimensional Confocal Micro X-ray Fluorescence (CμXRF)

Micro X-ray Fluorescence (CμXRF) is a revolutionary method that can be used to identify the chemistry of spongin-based skeletal fibers [12]. Using 3D CμXRF analysis, the distribution of bromine (as the main element in skeletal structures of verongiids [13]) and calcium have been visualised up to an absolute analysis depth of 1500 µm (**Figure 2**).

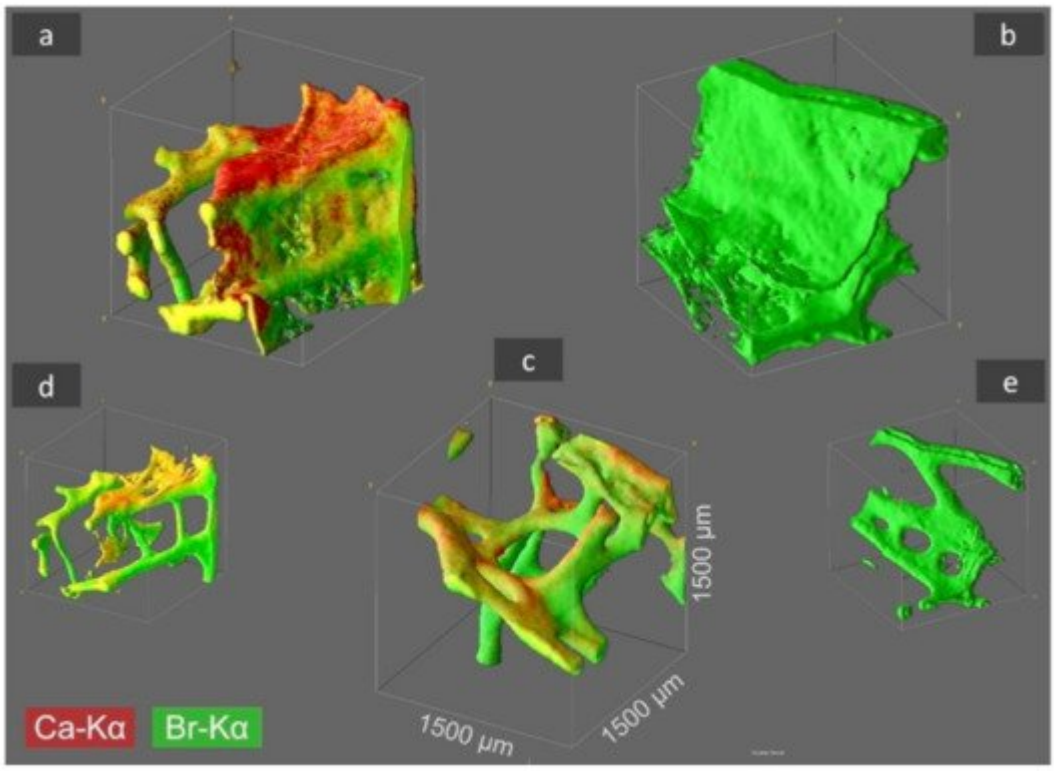

Figure 2. CμXRF analysis results of selected *I. basta* skeletal samples after treatment with distilled water (**a**), 3 M HCl (**b**), and 10% NaOH at 40 °C (**c**). The 3D distribution of Ca (red) and Br (green) is illustrated in the figure for an analyzed sample volume of 1.5 × 1.5 × 1.5 mm^3 (and locations with both elements are shown in a yellow coloration). By HCl treatment the Ca is removed from the skeletal structure (b), whereas by NaOH treatment both elements, Ca and Br, remain within the demosponge, however thin proteinaceous tissue layers between the sponge's skeleton are dissolved (c) and characteristic 3D chitinous construct remains present [14]. In figures (**d**,**e**) the sponge structure of (a,b) is depicted without the above-mentioned thin tissue layers, which was obtained by omitting the regions with very low signal intensity from data processing.

3D-CμXRF visualization of the samples demonstrated that the maximum Ca-Kα signal intensities of the original *I. basta* skeleton fragment treated with water and that after alkali treatment was 40 and 19 cps (counts per second), respectively. After the treatment of the same specimen with 3M HCl, the calcium in the skeletal scaffold was dissolved away and nearly no calcium was observed, resulting in a drastically reduced signal intensity of 2 cps, which is more than an order of magnitude lower compared with the calcium signal values of the two samples listed above. However, it seems that the different solution treatments have no significant effect on the absolute Br-Kα signal intensity with 38.0 cps (**Figure 2**a), 34.0 cps (**Figure 2**b), and 32.0 cps (**Figure 2**c), indicating, that each element is bound in different ways in the skeletal scaffolds.

Since the high fluorescence energy of the Br-Kα fluorescence lines allows obtaining signals from 1500 µm depth, the 3D visualization obtained from Br analysis does not only represent the surface morphologies but also the in-depth architecture of the sponge scaffolds. Thus, the 3D-CµXRF visualisation has been particularly useful to reveal the structural complexity of the *I. basta* skeletal scaffolds. However, in comparison to bromine, Ca is a much lighter element and therefore the energy of the Ca-Kα fluorescence lines appear with significantly lower energy. This results in a bigger cross-section dimension of the probing volume of Ca (28 µm for Ca-Kα, 16 µm for Br-Kα) and a much more limited measurement depth due to a more intensive absorption of the Ca fluorescence radiation by the sponge matrix. Consequently, the actual *I. basta* skeletal structure seems to be encircled by a Ca-containing "shell". This suggestion has been confirmed by observations of the same structures using scanning electron microscopy (SEM) (**Figure 3**a–d).

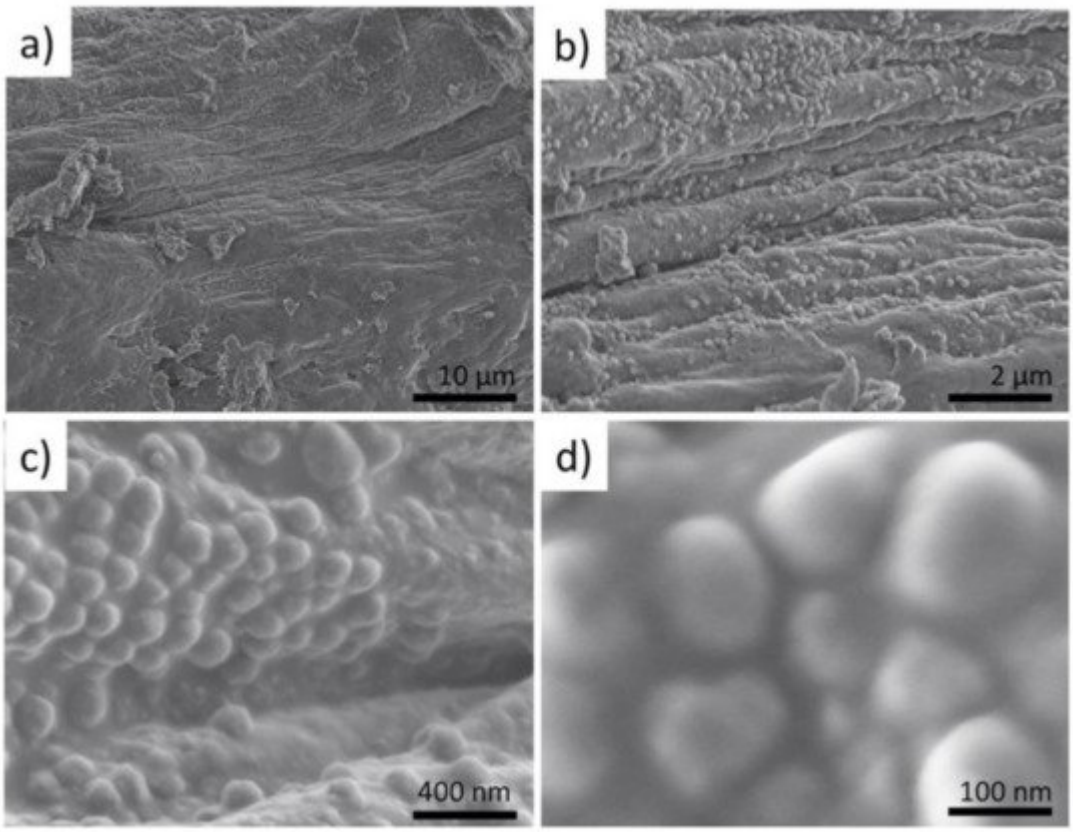

Figure 3. SEM images of the selected fragment treated with a distilled fragment of *I. basta* sponge skeletal fiber (**a**) show the presence of sphere-like nanoparticles (**b**–**d**).

3. Visualization of the Presence of Mineral Phase Using Electron Microscopy Methods

The micro-and nano-architecture of the *I. basta* skeleton (see **Figure 2**a), which consists of water-insoluble nanoparticles covering the surface of the skeletal fibers, have been revealed by energy dispersive spectroscopic (EDS) analysis carried out along with SEM imaging. The presence of Ca together with other elements typical for skeletal structures of verongiid sponges have been confirmed by this particular method [2] (**Figure 3**a). Similarly,

further investigations carried out using EDS analysis along with transmission electron microscopy (TEM) on the isolated nanoparticles also confirmed the localization of Ca within them (**Figure 4**b,c). These nanoparticles were found to be in nanocrystalline form (**Figure 5**).

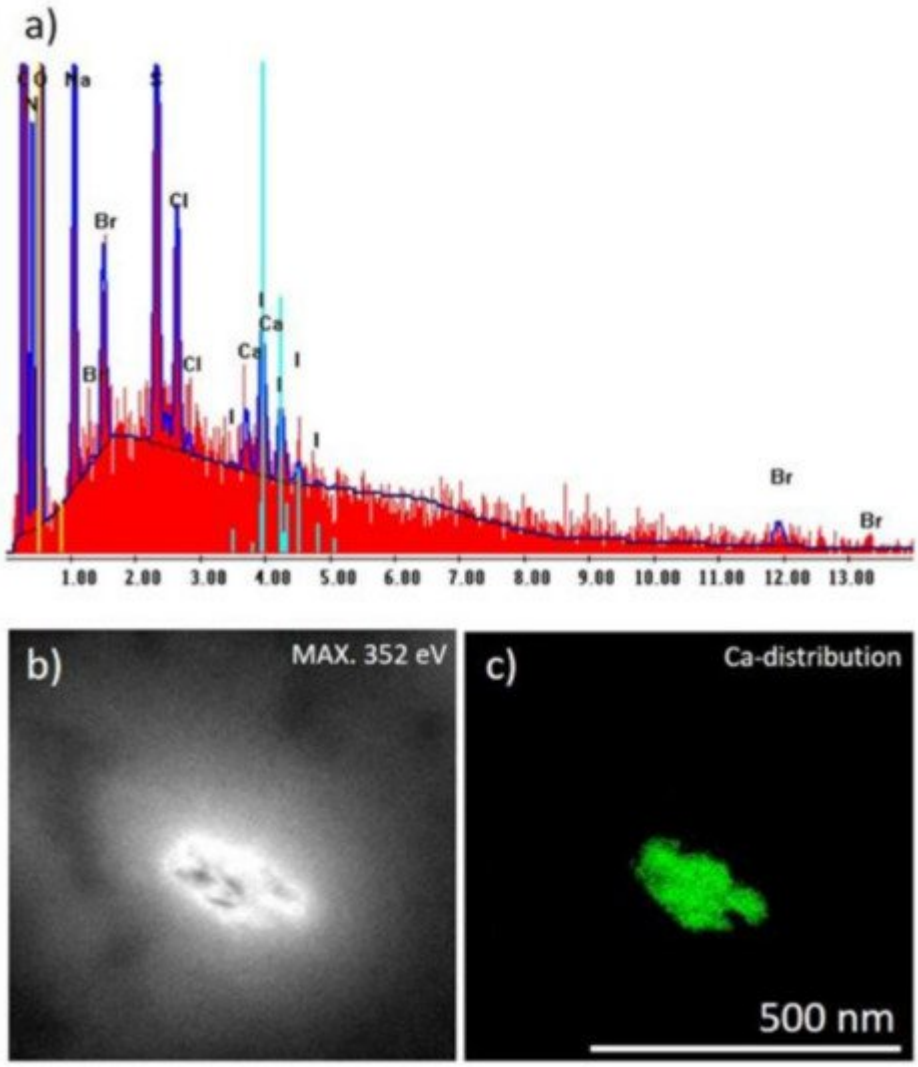

Figure 4. (**a**) EDS analysis of the *I. basta* skeletal fiber washed with distilled water demonstrating the atomic composition of this structure; (**b**) bright-field image of corresponding TEM image and (**c**) Ca distribution within the corresponding sample visualized in green color (colorization provided by the software to highlight electron diffraction signals of Ca atoms).

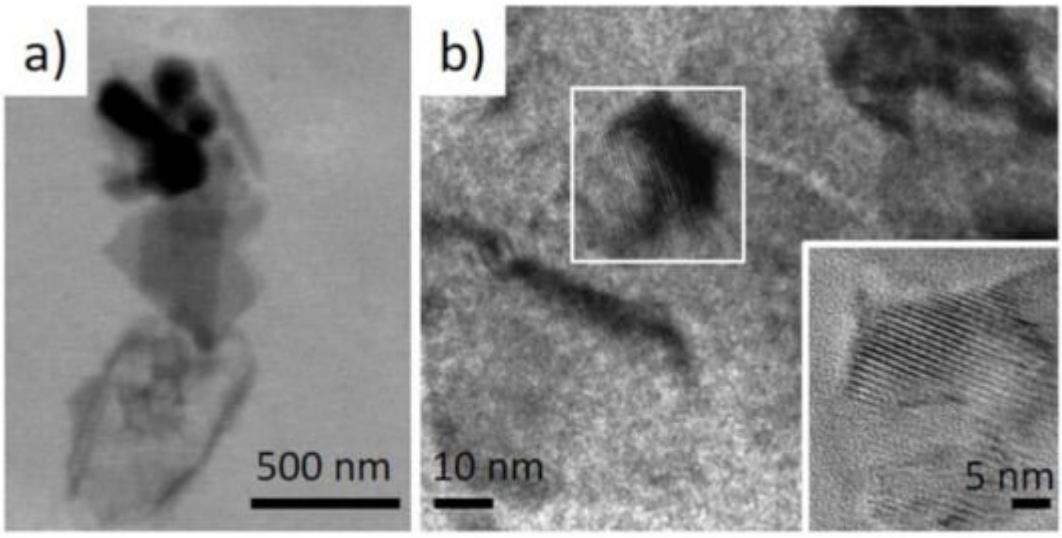

Figure 5. (**a**) low-resolution TEM image of the selected micro-fragment of the *I. basta* skeletal fiber-containing nanoparticles and (**b**) high-resolution TEM images showing their crystalline nature.

4. Identification of Calcite within *I. basta* Skeletal Fibres

The classical analytical methods such as X-ray diffraction (XRD), Fourier transforms infrared (FTIR), and Raman spectroscopy have been known to be useful for the identification of the mineral phases, such as calcium carbonate of biomineral origin [2][3][15][16]. Correspondingly, the presence of calcite in the studied *I. basta* samples revealed by the XRD method (CaCO3, ICSD PDF# 00-005-0586, space group R3c) (**Figure 6**). The lattice parameters of calcite were determined as a = (4.976 ± 0.002) Å and c = (16.981 ± 0.009) Å.

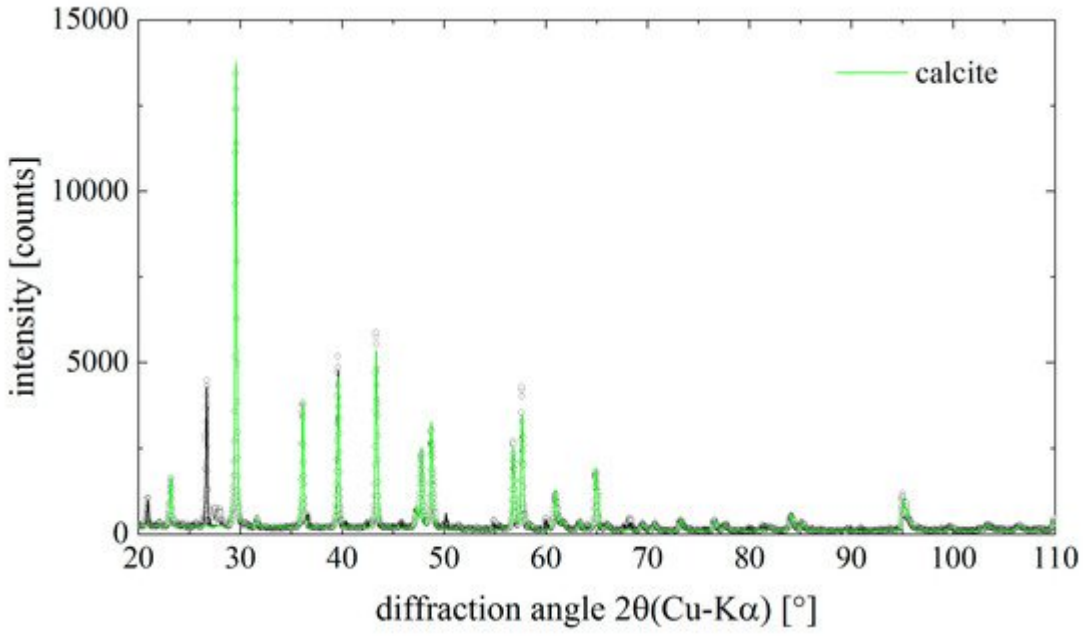

Figure 6. Diffraction pattern of the mineral phase isolated from chitinous skeletal fibers of *I. basta* demosponge. Dots are measured data points, the solid lines result from a Rietveld- (Pawley)-fit of the data. The contribution of

calcite to the total diffraction pattern is highlighted in green color. Calcite is the main component in the sample.

Along with calcite, quartz (SiO_2, ICSD PDF# 00-046-1045, space group $P3_221$) was found in the *I. basta* samples.

In addition to the XRD analysis, the calcite within the nanocrystalline mineral phase were identified infra-red and Raman spectroscopies. The FTIR band at 712–713 cm^{-1}, which was well visible in the investigated specimens which are characteristic for calcite standard (**Figure 7**) but also in agreement with the data reported previously for biogenic calcite [17].

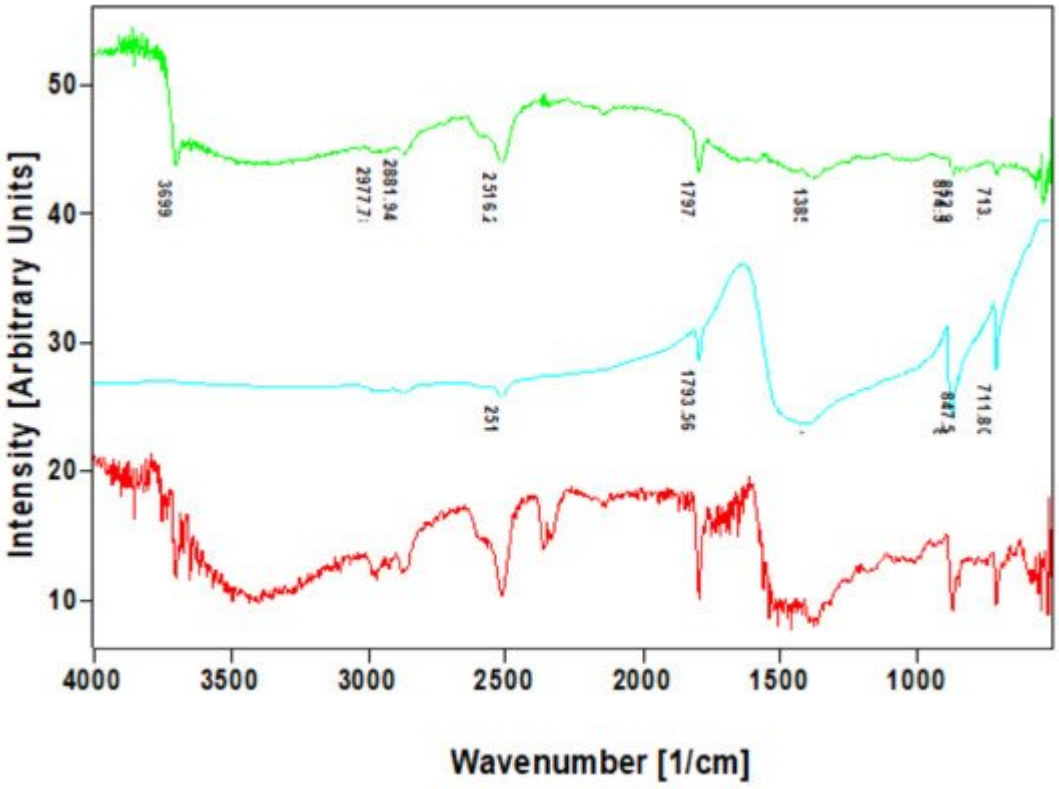

Figure 7. Comparative FTIR spectra of calcite standard (blue line) with that of nanocrystalline phases isolated from skeletal fibers of *I. basta* demosponges collected near Guam (USA) (red line) and in coastal waters of Australia (green line).

The data obtained using FTIR spectroscopy also correlated well with results from Raman spectroscopy analysis (**Figure 8**); which is in agreement with the Raman spectra of calcium carbonate phases [18][19].

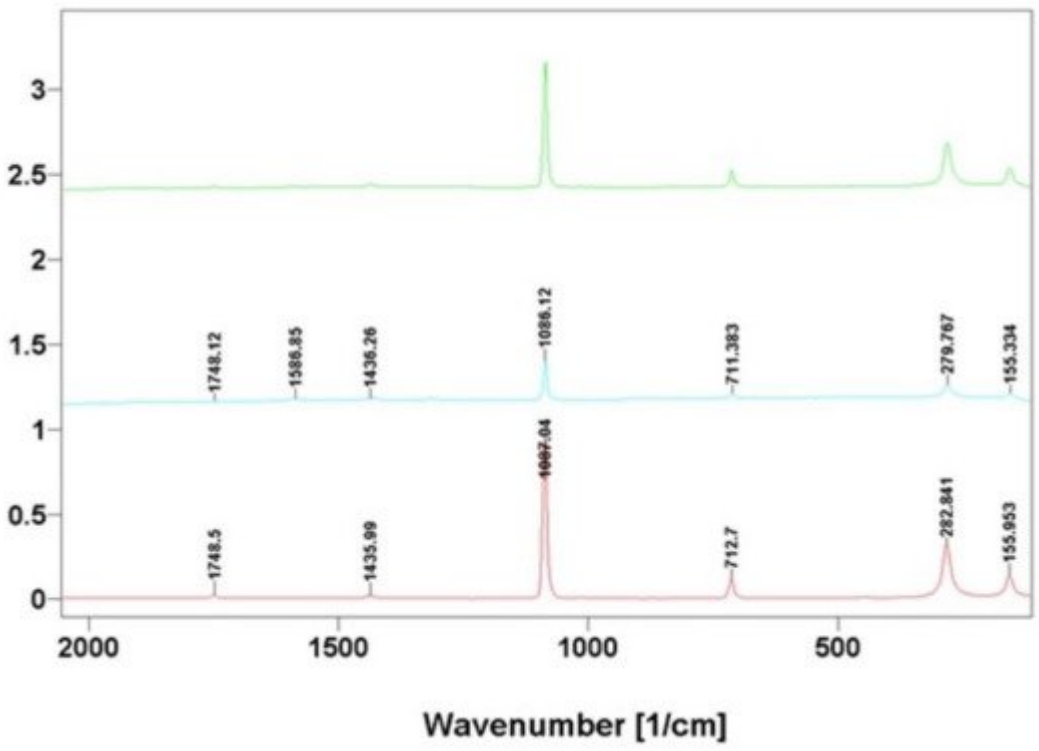

Figure 8. Comparative Raman spectra of calcite standard (blue line) with that of nanocrystalline phases isolated from skeletal fibers of *I. basta* demosponges collected near Guam (USA) (red line) and in coastal waters of Australia (green line).

5. Near Edge X-ray Fine Structure (NEXAFS) Features of Identified Mineral Phase

In order to gain insight into the nature of the structural components, the building-block picture for the ionic crystal of calcium carbonate was used. It is know that, a preliminary analysis of complex structures can be obtained within a building-block model, by which the structure is seen as an assembly of smaller pieces [37]. Those building blocks contribute independently to the total spectrum. In this way, specific spectral features can be correlated with contributions arising from individual functional groups. The convincing evidence that skeletal fibers of *I. basta* demosponge contains calcium carbonate as a mineral was obtained for the first time from NEXAFS C1s and Ca2p experiments. The NEXAFS in the regions of the C1s and the Ca2p edges are diagnostic for the identification of the calcium carbonate mineral.

In the mineral calcite, and its polymorphs (vaterite and aragonite), there is an ionic bond between the calcium cation and the planar anion $[CO_3]^{2-}$. Inside the anion, carbon and oxygen atoms are in a covalent bond. Thus, a stable flat group $[CO_3]^{2-}$ is a necessary element of calcite. Moreover, in calcite, calcium is in the immediate environment of 6 oxygen atoms which are close to octahedral. In vaterite, the calcium environment is also

consisting of 6 atoms and is similar to octahedral, which determines the strong similarity of the fine structure of Ca 2p spectra of these minerals [20].

In aragonite, the calcium environment is completely different and amounts to 9 oxygen atoms, and, accordingly, the fine structure of its Ca 2p spectrum is different from vaterite and calcite [20]. It is important to note that in calcium oxide CaO, the environment of calcium with oxygen is the undistorted octahedron and the fine structure of the Ca 2p spectrum of CaO is the same as of the calcite. The Ca 2p spectra themselves reflect only the symmetry of the nearest oxygen environment; therefore, the $[CO_3]^{2-}$ anion availability is evidence for the presence of calcite and its polymorphs. The narrow π * resonance (290.1–290.3 eV) in the NEXAFS C1s absorption spectrum demonstrates the presence of the planar group $[CO_3]^{2-}$ [21][22].

The NEXAFS in the regions of the C1s and the Ca2p edges are used for the identification of the calcium carbonate mineral (**Figure 9**). In calcite, the carbon atoms are in a planar CO_3 group, and the Ca atoms are in an octahedral coordination environment of the oxygen atoms. The presence of a carbonate peak at 290.28 eV in the C K-edge NEXAFS spectrum of the *I. basta* before and after treatment (**Figure 9** left) indicates that this peak is closely associated with carbonates (290.2 eV) [21].

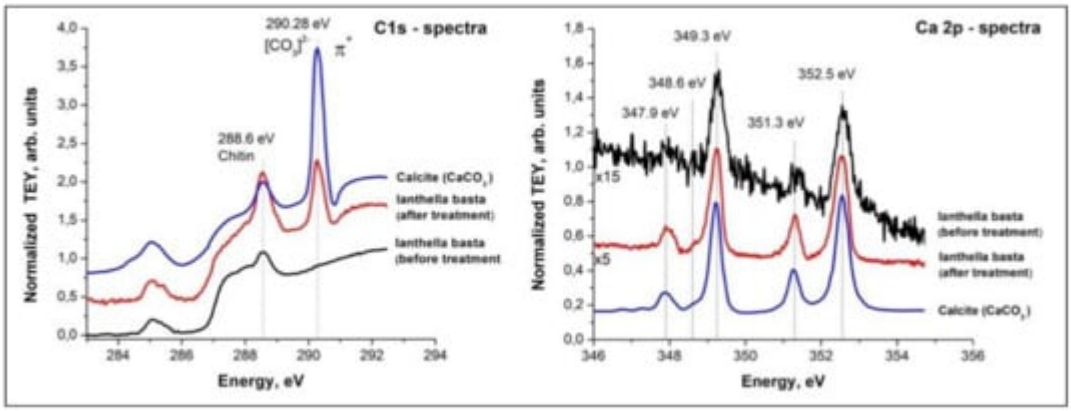

Figure 9. NEXAFS C1s (left) and Ca2p (right) spectra of *I. basta* skeletal fibers before and after NaOH treatment in comparison with calcite standard.

References

1. Ehrlich, H.; Bailey, E.; Wysokowski, M.; Jesionowski, T. Forced Biomineralization: A Review. Biomimetics 2021, 6, 46.
2. Ehrlich, H.; Brunner, E.; Simon, P.; Bazhenov, V.V.; Botting, J.P.; Tabachnick, K.R.; Springer, A.; Kummer, K.; Vyalikh, D.V.; Molodtsov, S.L.; et al. Calcite Reinforced Silica-Silica Joints in the Biocomposite Skeleton of Deep-Sea Glass Sponges. Adv. Funct. Mater. 2011, 21, 3473–3481.

3. Ehrlich, H.; Simon, P.; Carrillo-Cabrera, W.; Bazhenov, V.V.; Botting, J.P.; Ilan, M.; Ereskovsky, A.V.; Muricy, G.; Worch, H.; Mensch, A.; et al. Insights into Chemistry of Biological Materials: Newly Discovered Silica-Aragonite-Chitin Biocomposites in Demosponges. Chem. Mater. 2010, 22, 1462–1471.
4. Sethmann, I.; Wörheide, G. Structure and Composition of Calcareous Sponge Spicules: A Review and Comparison to Structurally Related Biominerals. Micron 2008, 39, 209–228.
5. Voigt, O.; Adamska, M.; Adamski, M.; Kittelmann, A.; Wencker, L.; Wörheide, G. Spicule Formation in Calcareous Sponges: Coordinated Expression of Biomineralization Genes and Spicule-Type Specific Genes. Sci. Rep. 2017, 7, 45658.
6. Shimizu, K.; Cha, J.; Stucky, G.D.; Morse, D.E. Silicatein Alpha: Cathepsin L-like Protein in Sponge Biosilica. Proc. Natl. Acad. Sci. USA 1998, 95, 6234–6238.
7. Shimizu, K.; Amano, T.; Bari, M.R.; Weaver, J.C.; Arima, J.; Mori, N. Glassin, a Histidine-Rich Protein from the Siliceous Skeletal System of the Marine Sponge Euplectella, Directs Silica Polycondensation. Proc. Natl. Acad. Sci. USA 2015, 112, 11449–11454.
8. Povarova, N.V.; Barinov, N.A.; Baranov, M.S.; Markina, N.M.; Varizhuk, A.M.; Pozmogova, G.E.; Klinov, D.V.; Kozhemyako, V.B.; Lukyanov, K.A. Efficient Silica Synthesis from Tetra(Glycerol)Orthosilicate with Cathepsin- and Silicatein-like Proteins. Sci. Rep. 2018, 8, 16759.
9. Ehrlich, H. Chitin and collagen as universal and alternative templates in biomineralization. Int. Geol. Rev. 2010, 52, 661–699.
10. Ehrlich, H.; Krautter, M.; Hanke, T.; Simon, P.; Knieb, C.; Heinemann, S.; Worch, H. First Evidence of the Presence of Chitin in Skeletons of Marine Sponges. Part II. Glass Sponges (Hexactinellida: Porifera). J. Exp. Zool. B Mol. Dev. Evol. 2007, 308, 473–483.
11. Wysokowski, M.; Jesionowski, T.; Ehrlich, H. Biosilica as a Source for Inspiration in Biological Materials Science. Am. Mineral. 2018, 103, 665–691.
12. Tsurkan, D.; Simon, P.; Schimpf, C.; Motylenko, M.; Rafaja, D.; Roth, F.; Inosov, D.S.; Makarova, A.A.; Stepniak, I.; Petrenko, I.; et al. Extreme Biomimetics: Designing of the First Nanostructured 3D Spongin–Atacamite Composite and Its Application. Adv. Mater. 2021, 33, 2101682.
13. Muzychka, L.; Voronkina, A.; Kovalchuk, V.; Smolii, O.B.; Wysokowski, M.; Petrenko, I.; Youssef, D.T.A.; Ehrlich, I.; Ehrlich, H. Marine Biomimetics: Bromotyrosines Loaded Chitinous Skeleton as Source of Antibacterial Agents. Appl. Phys. A 2021, 127, 15.
14. Brunner, E.; Ehrlich, H.; Schupp, P.; Hedrich, R.; Hunoldt, S.; Kammer, M.; Machill, S.; Paasch, S.; Bazhenov, V.V.; Kurek, D.V.; et al. Chitin-Based Scaffolds Are an Integral Part of the Skeleton of the Marine Demosponge Ianthella basta. J. Struct. Biol. 2009, 168, 539–547.

15. Sun, J.; Wu, Z.; Cheng, H.; Zhang, Z.; Frost, R.L. A Raman Spectroscopic Comparison of Calcite and Dolomite. Spectrochim. Acta Part A Mol. Biomol. Spectrosc. 2014, 117, 158–162.
16. Li, H.; Sun, C.-Y.; Fang, Y.; Carlson, C.M.; Xu, H.; Ješovnik, A.; Sosa-Calvo, J.; Zarnowski, R.; Bechtel, H.A.; Fournelle, J.H.; et al. Biomineral Armor in Leaf-Cutter Ants. Nat. Commun. 2020, 11, 5792.
17. Falini, G.; Fermani, S.; Gazzano, M.; Ripamonti, A. Structure and Morphology of Synthetic Magnesium Calcite. J. Mater. Chem. 1998, 8, 1061–1065.
18. Urmos, J.; Sharma, S.K.; Mackenzie, F.T. Characterization of Some Biogenic Carbonates with Raman Spectroscopy. Am. Mineral. 1991, 76, 641–646.
19. De La Pierre, M.; Carteret, C.; Maschio, L.; André, E.; Orlando, R.; Dovesi, R. The Raman Spectrum of CaCO3 Polymorphs Calcite and Aragonite: A Combined Experimental and Computational Study. J. Chem. Phys. 2014, 140, 164509.
20. Stöhr, J. NEXAFS Spectroscopy; Springer: Berlin/Heidelberg, Germany, 1992.
21. Benzerara, K.; Yoon, T.H.; Tyliszczak, T.; Constantz, B.; Spormann, A.M.; Brown, G.E. Scanning Transmission X-ray Microscopy Study of Microbial Calcification. Geobiology 2004, 2, 249–259.
22. Benzerara, K.; Menguy, N.; López-García, P.; Yoon, T.-H.; Kazmierczak, J.; Tyliszczak, T.; Guyot, F.; Brown, G.E., Jr. Nanoscale Detection of Organic Signatures in Carbonate Microbialites. Proc. Natl. Acad. Sci. USA 2006, 103, 9440–9445.
23. Madix, R.J.; Solomon, J.L.; Stöhr, J. The Orientation of the Carbonate Anion on Ag(110). Surf. Sci. 1988, 197, L253–L259.